

Two stripped envelope supernovae with circumstellar interaction

- but only one really show it.

J. Sollerman¹ & Co.^{2,3} including e.g., (not currently in order) C. Fremling, S. Schulze, C. Barbarino, C. Fransson, I. Sfaradi, A. Horesh, L. Tartaglia?, E. Kool, S. Yang, ...

¹ Department of Astronomy, The Oskar Klein Center, Stockholm University, AlbaNova, 10691 Stockholm, Sweden

² Division of Physics, Mathematics and Astronomy, California Institute of Technology, Pasadena, CA 91125, USA

³

Abstract

Context. We present observations of SN 2019tsf (ZTF19ackjszs) and SN 2019oys (ZTF19abucwzt). These two stripped envelope (SE) Type Ib supernovae (SNe) suddenly showed a (re-)brightening in their late light curves. We investigate this in the context of circumstellar (CSM) interaction with previously ejected material, a phenomenon that is unusual among SE SNe.

Aims. We use our follow-up photometry and spectroscopy for these supernovae to demonstrate the presence of CSM interaction, estimate the properties of the CSM and discuss why the signals are so different for the two objects.

Methods. We present and analyse observational data, consisting of optical light curves and spectra. For SN 2019oys we also have detections in radio as well as limits from UV and X-rays.

Results. Both light curves show spectacular re-brightening after about 100 days. In the case of SN 2019tsf, the re-brightening is followed by a new epoch of decline, and the spectra never show signs of narrow emission lines that would signal CSM interaction. On the contrary, SN 2019oys made a spectral makeover from a Type Ib to a spectrum clearly dominated by CSM interaction at the light-curve brightening phase. The deep Keck spectra reveal a plethora of high ionization coronal lines and the triggered radio observations show strong detections.

Conclusions. The rather similar light curve behaviour - with a late linear re-brightening - of these two Type Ib SE SNe indicate CSM interaction as the powering source. For one of our SNe the evidence for a phase where the ejecta hit H-rich material, likely ejected from the progenitor star, is conspicuous. We observe strong narrow lines of H and He, but also a plethora of high ionization coronal lines revealing shock interaction. The evidence is corroborated by detections in radio. On the contrary, for SN 2019tsf, we find little evidence in the spectra for any CSM interaction.

Key words. supernovae: general – supernovae: individual: ZTF19ackjszs, SN 2019tsf, ZTF19abucwzt, SN 2019oys

1. Introduction

Core-collapse (CC) supernovae (SNe) are explosions of massive stars ($\gtrsim 8 M_{\odot}$) reaching the end of their stellar life-cycles. The variety of CC SNe is largely determined by the progenitor mass at the time of CC, but also by the mass-loss history leading up to the explosion. Hydrogen-poor CC SNe originate from massive progenitor stars that have lost most - or even all - of their H envelopes prior to explosion. These include Type IIb SNe (some H left), SNe Ib (no H, some He), SNe Ic (neither H nor He) as well as superluminous supernovae of Type I (SLSNe-I). Collectively, SNe IIb, Ib and Ic are called stripped-envelope (SE) SNe.

There are few observational constraints on mass loss for very massive stars, and the processes involved are poorly understood. Models argue that for a star to experience enough mass loss to become a SE SN, either strong stellar winds from very massive progenitors ($\gtrsim 30 M_{\odot}$, Groh et al. 2013), or binary interactions are needed. In the binary scenario the progenitors can be of somewhat lower mass ($\lesssim 20 M_{\odot}$, e.g., Yoon 2015).

Evidence is emerging that a large fraction of SE SNe originate from binary systems. Both detailed studies of individual SNe, like the Type IIb SNe 1993J (Nomoto et al. 1993; Maund & Smartt 2009) and 2011dh (Ergon et al. 2014, 2015), as well as sample studies (Cano 2013; Taddia et al. 2015; Lyman et al.

2016; Taddia et al. 2018; Prentice et al. 2019) indicate ejecta masses of just a few M_{\odot} . This is too low to be consistent with the most massive stars that lose their envelopes due to winds (Groh et al. 2013). However, in either case, there must be ample material from the progenitor surrounding the stripped star at the time of explosion. The composition and distribution of this material contain information about the mass-loss process, as many of the binary stripping scenarios couple the phases of mass-transfer to the original binary separation (e.g., Smith 2014). The observational signatures would be evidence that the SN ejecta run into this circumstellar envelope material during some phase of the supernova evolution. This interaction between the ejecta and the circumstellar material (CSM) can produce a significant contribution to the total luminosity (e.g., Chevalier & Fransson 2017).

Evidence for the presence of significant CSM has been found in some SE SNe of Type IIb; late spectra of SN 1993J showed a broad flat-topped hydrogen signature that can be explained as due to CSM interaction (Matheson et al. 2000; Houck & Fransson 1996). Similar signatures were present in ZTF18aalxas (Fremling et al. 2019). The past years of observations have also revealed cooling phases similar to those observed in the early light curves (LC) of SNe IIb among other SE SN subtypes, indicating extended material outside these otherwise compact pro-

genitors. Examples include the Type Ic SNe iPTF15dtg (Taddia et al. 2016) and iPTF14gqr (De et al. 2018), where the latter also showed so-called flash spectroscopy signatures indicative of close-by CSM (Gal-Yam et al. 2014). Moreover, several SLSNe-I have been found to enter into an interaction phase with H-rich CSM in the years after explosion. In these cases, broad H features developed over time (Yan et al. 2017). Finally, SN 2014C (Milisavljevic et al. 2015), SN 2017ens (Chen et al. 2018) and SN 2017dio (Kuncarayakti et al. 2018a) constitute three very rare cases where SE SNe have spectroscopically metamorphosed into CSM interacting Type II supernovae, revealing the presence of external CSM at later phases.

In this paper we present two SE SNe that were discovered after peak in their evolution, but that both after a few months started to (re-)brighten. The extra power needed for such a light curve evolution is presumably CSM interaction simply because none of the other powering mechanisms at play at later phases are likely to display such a behaviour (see e.g., Sollerman et al. 2019 for a discussion and assessment of some of the scenarios; magnetar, radioactivity, accretion).

The paper is organized as follows. In Sect. 2 we present the observations, including optical photometry and spectroscopy but also some space-based observations and radio data. Section 3 presents a discussion of the similarities and differences between the two objects and finally Sect. 4 presents our conclusions, and contains a discussion where we put our observations in context with other SNe.

2. Observations

2.1. Detection and classification

SN 2019oys (a.k.a. ZTF19abucwzt) was first detected on 2019 August 28 (JD = 2458723.98), with the Palomar Schmidt 48-inch (P48) Samuel Oschin telescope as part of the Zwicky Transient Facility (ZTF) survey (Bellm et al. 2019; Graham et al. 2019). It was reported to the TNS¹ on Aug. 29. The first detection is in g band, with a host-subtracted magnitude of 19.14 ± 0.12 mag, at the J2000.0 coordinates $\alpha = 07^h07^m59.26^s$, $\delta = +31^\circ39'55.3''$. This transient was subsequently also reported to the TNS by several other surveys; in September by Gaia and ATLAS and in November by Pan-STARRS.

SN 2019oys is positioned in a spiral galaxy with the name CGCG 146-027 NED01 that had a reported redshift of $z = 0.0165$. Using a flat cosmology with $H_0 = 70 \text{ km s}^{-1} \text{ Mpc}^{-1}$ and $\Omega_m = 0.3$ this corresponds to a distance of 73.2 Mpc when accounting for the NED infall model.

Our first ZTF photometry for SN 2019tsf (a.k.a. ZTF19ackjszs) was obtained on 2019 October 29 (JD = 2458786.03) with the P48. The first detection is in r band, with a host-subtracted magnitude of 17.40 ± 0.06 mag, at $\alpha = 11^h08^m32.80^s$, $\delta = -10^\circ28'54.4''$ (J2000.0). This transient was first reported to the TNS by Gaia on Oct. 30 (Hodgkin et al. 2019), and later also by ATLAS, ZTF and Pan-STARRS.

The host galaxy of SN 2019tsf is NGC 3541, which has a well established redshift of $z = 0.021$ and a redshift independent distance of 83.9 Mpc from Springob et al. (2014).

None of these transients had constraining pre-explosion detections. For SN 2019tsf, Gaia reported upper limits from

August, 3 months prior to discovery, and SN 2019oys had similarly limits from end of May. It seems that both SNe exploded when in Solar conjunction and were only discovered while already on the decline. The typical rise time for a Type Ib supernova is ~ 22 days (Taddia et al. 2015), so it is likely that we missed both the rise and the peak. Given the absolute r -band magnitude at discovery, they were likely found within a month from peak (compare Taddia et al. 2018, their fig. 7). This is also consistent with the classification spectra. Since we do not know the time of explosion, throughout this paper we will always discuss both transients with phases with respect to first detection, as given above.

We classified SN 2019oys based on a spectrum obtained on 2019 Aug. 29 with the Palomar 60-inch telescope (P60; Cenko et al. 2006) equipped with the Spectral Energy Distribution Machine (SEDM; Blagorodnova et al. 2018; Rigault et al. 2019). It was the only spectrum we obtained of this transient in 2019, and we reported the classification to TNS as a Type Ib supernova. For SN 2019tsf, the classification was done by ePESSTO+ (Malesani et al. 2019). They report a Type Ib supernova close to max at a redshift of about 0.03, with no note of the NGC galaxy host.

Since both of these supernovae were found declining, no additional attention was given to them for the next ~ 100 days, but they were photometrically monitored as part of ZTF routine observations. The interest emerged again once the light curves all of a sudden started brightening at later phases.

2.2. Optical photometry

Following the discoveries, we thus obtained regular follow-up photometry during the declining phase in g and r band with the ZTF camera (Dekany et al. 2020) on the P48. Later on, after rebrightening started, we also obtained triggered photometry in gri with the SEDM on the P60. Lightcurves from the P48 come from the ZTF pipeline (Masci et al. 2019). Photometry from the P60 were produced with the image-subtraction pipeline described in Fremling et al. (2016), with template images from the Sloan Digital Sky Survey (SDSS; Ahn et al. 2014). This pipeline produces PSF magnitudes, calibrated against SDSS stars in the field. All magnitudes are reported in the AB system.

In our analysis we have corrected all photometry for Galactic extinction, using the Milky Way (MW) color excess $E(B - V)_{\text{MW}} = 0.06$ mag toward the position of SN 2019tsf and $E(B - V)_{\text{MW}} = 0.08$ mag toward the position of SN 2019oys (Schlafly & Finkbeiner 2011). All reddening corrections are applied using the Cardelli et al. (1989) extinction law with $R_V = 3.1$. No further host galaxy extinction has been applied, since there is no sign of any NaID absorption in any of our spectra. The light curves are shown in Fig. 1.

For SN 2019oys, the initial decline lasted at least 70 days (again, this is past discovery in the observers frame). It declined quickly in the r band at a rate of 3.1 mag per 100 days, and somewhat slower at 1.8 mag per 100 days in the g band, thus becoming less red with time. We then have a gap in our observations, and when imaging was resumed again after about a month in December 2019, it was clear that the decline had not continued, but that in fact the light curve was now rebrightening. Once this was realized in mid-January 2020, a more intense follow-up was activated.

SN 2019tsf had a r -band decline over 65 days with a more normal (for SE SNe) rate of 1.4 mag per 100 days. The g -band light curve is more sparse, but is again shallower. For this supernova we can more clearly see the onset of the brightening after

¹ <https://wis-tns.weizmann.ac.il/>

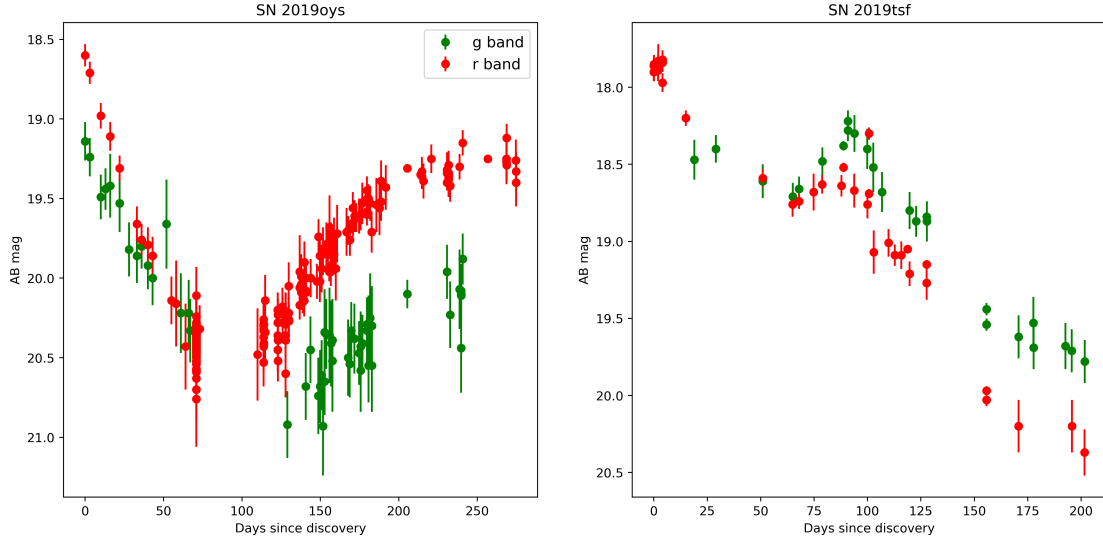


Figure 1: Lightcurves of SN 2019oys (left) and SN 2019tsf (right) in g (green symbols) and r (red) band. These are observed (AB) magnitudes plotted versus observer frame time in days since first detection. Both these Type Ib SNe showed a dramatic increase in brightness after months of decline, and in the case of SN 2019oys that rebrightening continued over more than 100 days. *Jesper: I will add arrows to show epochs of spectroscopic observations as well.*

70 days, the g -band light curve rises most clearly by 0.46 mags over the next 26 days, whereas the r band increases by slightly more than 0.1 mag.

2.3. Swift-observations

2.3.1. UVOT photometry

For SN 2019oys, which did show clear evidence for CSM interaction (see below), we triggered a series of ultraviolet (UV) and optical photometry observations with the UV Optical Telescope onboard the Neil Gehrels *Swift* observatory (*UVOT*; Gehrels et al. 2004; Roming et al. 2005). Our first *Swift-UVOT* observation was performed on 2020 March 9 and provided detections in all the bands. However, upon inspection it is difficult to assess to what extent the emission is actually from the supernova itself, or if it is diffuse emission from the surroundings. The last u -band detection appears to be real and point-like ($u = 20.16^{+0.30}_{-0.23}$ mag (AB) at MJD=58986.31), but for the remaining bands we would need to await template subtracted images to get reliable photometry. Unfortunately, the SN was still brightening as it went behind the Sun.

2.3.2. X-rays

With *Swift* we also used the onboard X-Ray Telescope (XRT; Burrows et al. 2005). We used online analysis tools (Evans et al. 2009) to search for X-ray emission at the location of SN 2019oys. Combining the five epochs taken in March 2020 amounts to a total XRT exposure time of 12 251 s (3.4 h), and provides a marginal detection with $16.7^{+3.5}_{-2.8} \times 10^{-3}$ counts s^{-1} between 0.3 and 10 keV. However, again it is not possible to assess if this is emission from the transient or from the host galaxy. We can conservatively treat this as an upper limit on the possible X-ray luminosity of the supernova itself. If we assume a power-law spectrum with a photon index of $\Gamma = 2$ and a Galactic hydrogen column density of 9.3×10^{20} cm^{-2} (HI4PI Collaboration et al. 2016) this would correspond to an unabsorbed 0.3–10.0 keV flux of 7.5×10^{-13} erg cm^{-2} s^{-1} . At the

luminosity distance of SN 2019oys this corresponds to a luminosity of $L_X < 4.7 \times 10^{41}$ erg s^{-1} at an epoch of ~ 200 rest-frame days since discovery.

2.4. Optical spectroscopy

Spectroscopic follow-up was conducted with SEDM mounted on the P60. Further spectra were obtained with the NOT using the A. Faint Object Spectrograph (ALFOSC), with the Keck-I telescope using the Low Resolution Imaging Spectrograph (LRIS; Oke et al. 1994), and with the Device Optimized for the LOW RESOLUTION (DOLORES) on Telescopio Nazionale Galileo (TNG). A log of the spectral observations is provided in Table 1, which includes 19 epochs of spectroscopy (9 for SN 2019tsf and 10 for SN 2019oys). Two of the NOT spectra were obtained with a somewhat higher resolution than we normally use (grism 8 instead of grism 4) to probe the width of the narrower lines. These observations were taken for SN 2019oys on days 167 and 243. The `LPipe` reduction pipeline (Perley 2019) was used to process the LRIS data. SEDM spectra were reduced using the pipeline described by Rigault et al. (2019) and the spectra from La Palma were reduced using standard pipelines and procedures for each telescope and instrument. All spectral data and corresponding information will be made available via WISeREP² (Yaron & Gal-Yam 2012).

2.5. Radio observations

Radio observations of the field of SN 2019oys were conducted using the Arcminute Microkelvin Imager - Large Array (AMI-LA; Zwart et al. 2008; Hickish et al. 2018). AMI-LA is an interferometer made up of eight 12.8 m antennas which operates with a 5 GHz bandwidth around a central frequency of 15.5 GHz. We conducted our first two AMI-LA observations of SN 2019oys on September 19 and 23, 2019. Initial data reduction, flagging, and calibration of the phase and flux, was carried out using a

² <https://wiserep.weizmann.ac.il/>

customized AMI data reduction software package. Phase calibration was done using interleaved observations of J0714+3534, while absolute flux calibration was achieved against 3C286. Additional flagging was performed using CASA.

The first two radio observations resulted in detections of a source at the phase center with an estimated flux of 0.35 mJy at 15.5 GHz, but with no apparent flux evolution. Following the spectacular coronal line spectrum obtained for SN 2019oys at the Keck telescope, providing strong evidence for CSM interaction, we triggered AMI-LA again on March 6, 2020. This observation provided a strong detection of the SN with a significantly higher flux of 9 mJy at 15.5 GHz, and the radio image is shown in the inset of the radio lightcurve in Fig. 2.

We also observed the field of SN 2019oys with the Karl G. Jansky Very Large Array (VLA) on March 16 2020³, while the VLA was in C configuration. The observations were performed in the S- (3 GHz), C- (5 GHz), X- (10 GHz), Ku- (15 GHz), K- (22 GHz) and Ka- (33 GHz) bands. We report here a spectral radio peak of $F_\nu = 21.5 \pm 1.0$ mJy at a frequency $\nu = 23.5 \pm 1.3$ GHz. The log of the radio observations and measurements is provided in Table 2. We continue monitoring SN 2019oys with the VLA.

3. Discussion

3.1. Light curves

The g - and r -band LCs of our two SNe are displayed in Fig. 1. We do have some complementary photometry also in other bands, mostly in the i band. These data are not plotted here for clarity, but are provided in the data-files released with the paper. The general behaviour of the LCs was already discussed in Sect. 2.2, and the main characteristic is of course the linear decline which is suddenly turned into a rebrightening. In Fig. 3 we show both LCs together in absolute magnitudes (here in the r band). This shows that SN 2019tsf is more luminous than SN 2019oys by almost a magnitude at discovery, and remains brighter until about 150 days later, when the prolonged rebrightening of SN 2019oys catch up. The magnitudes in Fig. 3 are in the AB system and have been corrected for distance modulus and MW extinction, and are plotted versus rest frame days past discovery. For comparison we have also included a typical Type Ib supernova, iPTF13bv from Fremling et al. (2016). This SN LC has been shifted by about two weeks for the maximum brightness to coincide with the discovery of our two SNe, and the distance and MW extinction have been taken from Fremling et al. (2016). The maximum brightness for iPTF13bv is similar to what we see at discovery for our two SNe, but after the diffusion phase the normal Type Ib fades faster. There is more late time photometry available for iPTF13bv, and the line in the figure connects smoothly to these data at about 200 days when iPTF13bv is much fainter than SNe 2019oys and 2019tsf. Our SNe clearly show very different LCs, and this is further discussed in Sect. 4.

We do not have enough photometric bands to construct a proper bolometric LC. We caution therefore that the strong brightening for the r band in SN 2019oys is to a large extent due to line emission in $H\alpha$. The $g - r$ color got steadily bluer during the decline of the light curve, while in the rising phase the color is again quite red. Between 150 and 172 days, $H\alpha$ increased from $\sim 60\%$ to $\sim 72\%$ of the r -band flux. This is reminiscent of the LC of the Type IIn SN 2006jd, where the r -band

flux reached a minimum at ~ 190 days, and then again brightened by ~ 1 mag, reaching a peak ~ 500 days after discovery (Stritzinger et al. 2012, their fig. 5). Also in this case was the evolution in the other bands less dramatic. The quasi-bolometric light curve of SN 2006jd showed a flat behaviour and later a decline during this period (Stritzinger et al. 2012, their fig. 9). A difference between SN 2019oys and SN 2006jd is that the dip in the r -band is more shallow and the minimum occurs at a later epoch for SN 2006jd.

3.2. Spectroscopy

For SN 2019tsf the classification spectrum revealed a Type Ib supernova (Malesani et al. 2019, Sect. 2.1). When we run SNID (Blondin & Tonry 2007) on this spectrum, the best match is SN 2008D, a well monitored Type Ib. We show this comparison in Fig. 4. The next spectrum was only obtained more than two months later, after the brightening, with the Nordic Optical Telescope (NOT) using ALFOSC (Table 1). The aim of this second spectrum was of course to search for evidence for CSM interaction that could explain the rising light curve. As can be seen in the spectral sequence (Fig. 4), no such evidence was found. We continued the spectroscopic campaign with spectra from P60, TNG, Keck and NOT - until the SN faded out of spectroscopic sight. The spectral evolution was quite slow - no significant evolution is apparent in the sequence from 80 to 180 days from discovery. In Fig. 4 we also compare the late spectra of SN 2019tsf with that of another ZTF supernova, the Type Ib SN 2019vsi. That spectrum was also obtained with NOT+ALFOSC about 80 days past discovery and show great similarity to the spectra of SN 2019tsf. In the context of the comparison to SN 2019oys and evidence for CSM interaction, we see little spectroscopic evidence that SN 2019tsf interacted with a CSM.

On the contrary, SN 2019oys displayed a spectacular metamorphosis. The first classification spectrum displayed a Type Ib SN with no signs of CSM interaction. Again, SN 2008D provides the best match by SNID, as illustrated in Fig. 5. That spectrum of SN 2008D was obtained 6 days past max, and is again an indication that our SNe were discovered past peak, but not by much. Also SN 2019oys was basically ignored for a long time, it was not considered interesting enough for spectroscopic follow-up given the lack of a well-determined explosion date. When we realised the supernova was on the rise, we triggered first the NOT, which revealed a booming narrow-line dominated spectrum. This was completely unlike the first spectrum. Wondering whether we might have missed some of these narrow features in the early very low dispersion SEDM spectrum, we took another SEDM spectrum just a few days later - and again got an emission line dominated spectrum, with a particularly strong $H\alpha$ line. Whereas the SEDM spectra can not reveal the dense forest of narrow lines, the metamorphosis was clearly apparent also in this comparison. The spectral sequence displayed in Fig. 5 basically illustrates mainly this; the sudden transition from a Type Ib to what is better described as a Type IIn supernova. To properly showcase the evolution of the spectra on the re-brightening part of the light curve, we show these spectra in logarithmic scale in Fig. 6. This allows displaying our best spectra showing a sequence of dense narrow-line spectra rich in high-ionization coronal lines. This figure also includes a comparison to the spectacular coronal line supernova SN 2005ip. This particular spectrum is taken from Stritzinger et al. (2012). SN 2005ip was a supernova that displayed many similarities to SN 2019oys. It was first classified as a Type II supernova, although in hindsight it did display a number of narrow emission lines already close to dis-

³ DDT program VLA/20A-421; PI Horesh.

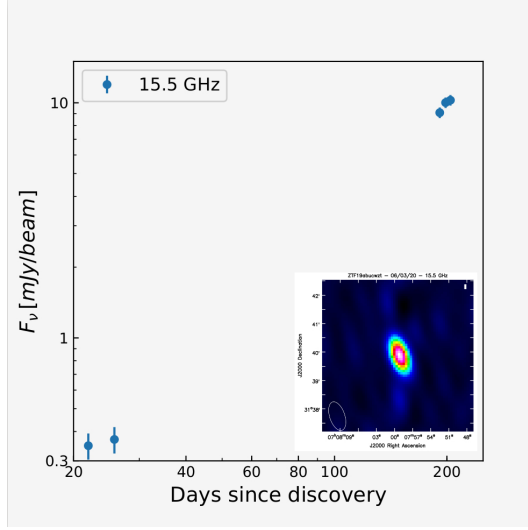


Figure 2: The radio light curve of SN 2019oys at 15.5 GHz as observed with AMI-LA. The inset in the lower right shows the radio image from AMI on March 6 2020, when the SN was detected at a level of 9 mJy. *Itai will make a nicer figure showing this?*

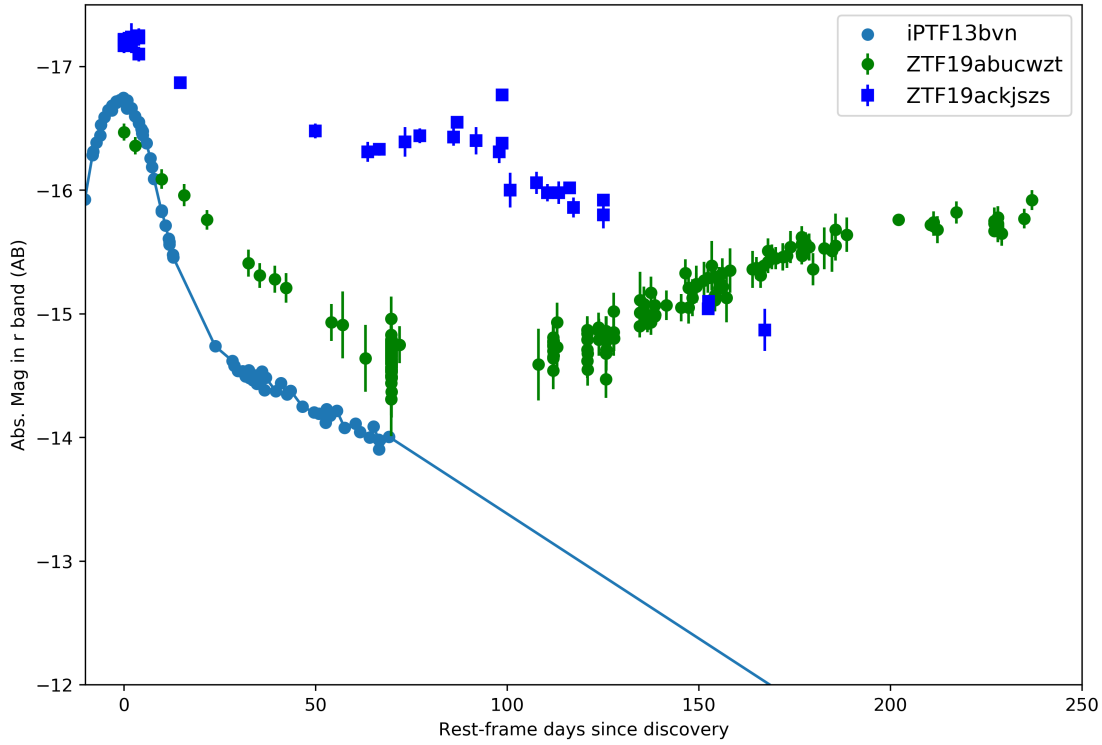


Figure 3: Light curves in absolute r -band magnitude (M_r) for our two supernovae. This accounts for distance modulus and MW extinction as discussed in the text, but no additional corrections for host extinction. In addition we have plotted the Type Ibn SN iPTF13bvn (Fremling et al. 2016), which is a typical radioactively powered stripped envelope supernova. *Jesper: Change ZTF names to SN names as labels. Bin the data on nightly basis here.*

covery. The light curve of SN 2005ip also missed the time of explosion, but did after about 200 days stop declining and entered more of a flat plateau, rather than the more dramatic increase in brightness that SN 2019oys delivered. The richness of coronal lines in SN 2005ip was unprecedented, and we make a direct comparison with the line identifications for this supernova from Smith et al. (2009) in Table 3. The spectrum of SN 2019oys is equally rich, displaying high ionization species such as for ex-

ample [Ar XIV], [Ne V] and [Fe XI]. We provide our own line identifications on the day 172 spectrum of SN 2019oys in Fig. 7.

Table 3 demonstrates that we detect and identify most of the multitude of emission lines also detected in SN 2005ip. Some notable exceptions are the [S II] $\lambda\lambda 6717, 6731$ that were strong in SN 20105ip, but are hardly detected in SN 2019oys. Overall the conditions present in the line forming region(s) must be quite similar between these two supernovae, these conditions were also studied in detail by Stritzinger et al. (2012) and earlier also

for the Type II_n SNe 1995N (Fransson et al. 2002) and 2010jl (Fransson et al. 2014). We discuss some diagnostics of the emission lines in the subsections below.

There are of course also some differences between the two above-mentioned SNe. Figure 6 shows that SN 2005ip displayed a broad component of H α , which is not present in SN 2019oys. This is a signature of the hydrogen-rich fast-moving ejecta that this Type II SN showed already from early times. SN 2019oys is instead a stripped envelope Type Ib SN, and such a supernova is more unlikely to metamorphose into a rich coronal line dominated transient.

In fact, less than a handful of SE SNe are known to have transitioned to CSM interacting objects, as mentioned in the introduction. SN 2017ens (Chen et al. 2018) was a very/super luminous Type Ic-BL that hit CSM after 150 days. It also displayed some coronal lines, but the light curve never rebrightened. This was a unique object, but indeed shares many properties with SN 2019oys. SN 2017dio (Kuncarayakti et al. 2018b) was a Type Ic that already from the start showed evidence for CSM interaction in terms of narrow emission lines. Rather than showing a spectacular change in spectral properties, it displayed a double nature with pseudo-continuum Type Ic spectral features with narrow Balmer lines à la Type II_n superimposed. Finally, we must also mention SN 2014C (e.g., Milisavljevic et al. 2015) which is by now a well studied SE SN that ran into CSM and which transformed from a Type Ib to a Type II_n SN, just like SN 2019oys. Also in this case, late time high resolution spectra revealed coronal lines. This small family of changing type SNe demonstrates the existence of nearby dense hydrogen-rich CSM close to - but not too close to - the stripped progenitor star, possibly from binary evolution and/or violent eruptions (Sun et al. 2020). Recently, SN 2018ijp was also interpreted as a SE SN with “delayed interaction” (Tartaglia et al. 2020, submitted).

Having mentioned several SNe showing a similar spectroscopic transition as did SN 2019oys, it is worth to remind that the LC of SN 2019oys is quite unique within this sample. Whereas SN 2005ip displayed a drastic change in decline when the CSM interaction started in earnest, the late light curve was more of a plateau than an actual rise. SNe 2014C, 2017dio and 2017ens also did not show signs of rebrightening, although for SN 2017dio it is possible that we missed the early phases.

3.2.1. Lyman-alpha fluorescence

The near-infrared (NIR) part of the spectrum shown in Fig. 7 displays a strong complex of lines. This has been seen previously in other SNe, in particular in SN 1995N (Fransson et al. 2002) and also for SN 2005ip (Fox et al. 2020, submitted), and has been explained as the result of fluorescence of Fe II by Ly α . In this process, electrons in the a^4D^e level of Fe II are excited to levels ~ 11.2 eV above the ground state by accidental resonances with the Ly α line (Johansson & Jordan 1984; Sigut & Pradhan 1998, 2003). The cascade to lower levels results in a UV line and a line in the NIR. Because these levels with high excitation temperatures are difficult to excite by thermal collisions, the presence of these NIR (and UV) lines is a strong signature of radiative pumping by Ly α . Although we do not have any UV spectra, especially our Keck spectra allow us to examine the NIR features.

Because of the multitude of Fe II lines all over the optical and NIR ranges, spectral simulations are required in order to identify the most likely and strongest transitions. We use the predicted line fluxes from the AGN simulations by Sigut & Pradhan (2003). The relative fluxes of all Fe II lines from the list of Sigut & Pradhan (2003) are shown as vertical bars in Fig. 7. While

the model identifies most of the Fe II lines in the range below ~ 5300 Å, which can be thermally excited, the interesting region is at $\sim 8400 - 9600$ Å, as can be seen in the lower panel of Fig. 7. In addition to the broad Paschen lines up to at least the $n = 14 \rightarrow 3$ transition, the Ca II triplet, and narrow [S III] $\lambda\lambda 9069, 9531$ lines, there are also a number of narrow lines from Fe II. While several of these are blended with lines from other ions, there are several lines which are not coming from lighter elements. In particular, the lines at 8927, 9123, 9132, 9176, 9178 Å can not be identified with other ions. These, together with the Fe II $\lambda 8451$ line, are also the ones expected to be strong in the model. The latter line is blended with a broad feature. While there is some contribution from high order Paschen lines, there is likely to be a strong contribution from O I $\lambda 8446$. There is thus strong evidence for narrow Fe II lines excited by Ly α .

3.2.2. Synthetic spectrum

To infer some basic properties of the CSM we have also calculated a synthetic spectrum of SN 2019oys. This was also useful to help in the identification of the lines in view of the line blending and many Fe II lines present. The synthetic spectrum is displayed in Fig. 8, together with the reddening corrected spectrum of SN 2019oys from day 172. The analysis assumes a two-zone model with separate densities for the narrow-line region and for the region responsible for the broader lines. We have assumed a blackbody background continuum with a temperature of 9900 K, while the temperature of the CSM was set to 15,000 K. The steep Balmer decrement with H α /H β ~ 8.5 requires a high density to produce optically thick Balmer lines. This depends on the temperature, and assuming 15,000 K requires a density of the broad line region of $\sim 4 \times 10^9$ cm $^{-3}$. For the narrow line region we instead assume a density 1×10^5 cm $^{-3}$, since this gives good agreement for the [O III] and Fe V lines.

4. Discussion and Conclusions

In this paper we have presented two SE Type Ib SNe whose light curves after months of decline suddenly started rebrightening. Such events are no doubt rare, and these discoveries heavily relies on the sky survey of ZTF which can not only discover many different kinds of transients, but also monitor them routinely enabling us to unravel unusual behaviour also at later epochs. One of the supernovae, SN 2019tsf, brighten only for a month, and then return to a declining phase of the light curve. Even though we managed to obtain high quality optical spectra at the time of the light curve bump, no clear spectral signatures of CSM interaction were seen. SN 2019oys, on the other hand, continued to rise until the end of this study, and the spectral metamorphosis is second to none of the few similar changing-type SE SNe known. The CSM interaction is evident and obvious and provide us with a plethora of diagnostic lines to investigate the surrounding environments. The dichotomy illustrated by this pair of SNe highlights a number of issues in contemporary supernova studies.

There is in fact an under-abundance of studies of what spectral signatures CSM interaction should provide. In the context of SLSNe-I, extraordinary luminous hydrogen-free transients, CSM interaction has been considered unlikely, partly based on the lack of narrow emission lines in their spectra (Mazzali et al. 2016), although that particular work focused more on modeling spectra without interaction rather than demonstrating that interaction could happen without spectral signatures. There are also SE SNe where interaction became more evident at late

stages, but where narrow emission lines never dominated the spectrum (e.g., Matheson et al. 2000, for SN 1993J). The discussion was exacerbated with the curious iPTF14hls, a Type II supernova with a spectacularly long-lived light-curve (Arcavi et al. 2017) where most of the run of the mill explanations for powering mechanisms did not work out, and where CSM interaction was probably the last scenario standing (Sollerman et al. 2019). Andrews & Smith (2018) explained the fact that such a CSM interaction did not reveal itself in the spectral evolution as due to a particular geometry hiding the interaction site, although actual modeling of such a mechanism remain unexplored.

Whereas the powering scenarios required to sustain long-lived or superluminous light-curves without displaying conspicuous spectral signals have been discussed in the literature, the problem is somewhat intensified by the two SNe presented in this work. They (re-)brighten significantly at late times, and it is quite challenging to envision any mechanism other than CSM interaction responsible for this behaviour. The well-monitored re-brightening allowed spectroscopic observations at the time of the interaction. We are then left with two stunningly different spectral signals - one CSM interaction scenario showing a load and clear Type II_n spectrum while the other simply do not. This reinforces the need for better understanding of the CSM scenario.

Returning to the light curves, and comparing to a prototypical SN Ib, such as iPTF13bvn in Fig. 3. On the one hand, the peak absolute magnitude of iPTF13bvn is in the same ballpark as the brightest points for our two SNe. Note again that this is not a bolometric LC, but in the r band. For iPTF13bvn, there were enough data to build and model a bolometric LC, and the conclusion was that it could be powered by $0.072 M_{\odot}$ of ^{56}Ni (Fremling et al. 2016). If we were to power the LCs of our SNe in the same way we would need more radioactive material. Assuming for example that we just missed the diffusion peaks of the SNe, we can match their LCs to that of iPTF13bvn by shifting them. Matching to the LC at about 50 days would require 0.2 and $0.6 M_{\odot}$ of ^{56}Ni , respectively, for the two supernovae, but the SN LCs could also have been affected by CSM powering already on the initial fading part.

In some sense, the interpretation of SN 2019oys in terms of CSM interaction as provided here puts it in the family of well explored SNe such as SNe 2015ip and 1988Z, and the formation of the coronal lines and the luminosity of the light curve can be understood in that context. However, this leaves open several fundamental questions, since SN 2019oys was not the explosion of a hydrogen-rich progenitor forming a Type II SN. Instead it was initially classified as a Type Ib, which is more similar to e.g., SN 2014C. Milisavljevic et al. (2015) discussed three different scenarios for the origin of such a CSM; a brief Wolf-Rayet phase, eruptive ejection or confinement of CSM by surrounding stars. There are many similarities between SN 2014C and SN 2019oys - like the coronal line spectrum and the FWHM of the intermediate with lines ($\sim 1500 \text{ km s}^{-1}$). In our case, it is unclear if this represents a real wind velocity of if the H and He lines could also be subject to electron scattering in the denser regions. We also note the difference in that SN 2014C showed a nebular spectrum with sawtooth shaped broad emission lines from the underlying ejecta, which is less obvious in the narrow line dominated spectrum of SN 2019oys. Investigating more of these systems will help us understand why some stripped stars engage in CSM interaction (while most do not) and why some reveal this conspicuously as did SN 2019oys, whereas others, like SN 2019tsf only provide a LC bump with no spectral CSM interaction signatures.

Acknowledgements. We thank Brad Cenko for guidance on the SWIFT data. Based on observations obtained with the Samuel Oschin Telescope 48-inch and the 60-inch Telescope at the Palomar Observatory as part of the Zwicky Transient Facility project. ZTF is supported by the National Science Foundation under Grant No. AST-1440341 and a collaboration including Caltech, IPAC, the Weizmann Institute for Science, the Oskar Klein Center at Stockholm University, the University of Maryland, the University of Washington, Deutsches Elektronen- Synchrotron and Humboldt University, Los Alamos National Laboratories, the TANGO Consortium of Taiwan, the University of Wisconsin at Milwaukee, and Lawrence Berkeley National Laboratories. Operations are conducted by COO, IPAC, and UW. The Oskar Klein Centre was funded by the Swedish Research Council. Partially based on observations made with the Nordic Optical Telescope, operated by the Nordic Optical Telescope Scientific Association at the Observatorio del Roque de los Muchachos, La Palma, Spain, of the Instituto de Astrofísica de Canarias. Some of the data presented here were obtained with ALFOSC. Some of the data presented herein were obtained at the W. M. Keck Observatory, which is operated as a scientific partnership among the California Institute of Technology, the University of California, and NASA; the observatory was made possible by the generous financial support of the W. M. Keck Foundation. This paper is partly based on observations made with the Italian Telescopio Nazionale Galileo (TNG) operated on the island of La Palma by the Fundación Galileo Galilei of the INAF (Istituto Nazionale di Astrofisica) at the Spanish Observatorio del Roque de los Muchachos of the Instituto de Astrofísica de Canarias. The SED Machine is based upon work supported by the National Science Foundation under Grant No. 1106171.

References

- Ahn, C. P., Alexandroff, R., Allende Prieto, C., et al. 2014, *ApJS*, 211, 17
- Andrews, J. E. & Smith, N. 2018, *MNRAS*, 477, 74
- Arcavi, I., Howell, D. A., Kasen, D., et al. 2017, *Nature*, 551, 210
- Bellm, E. C., Kulkarni, S. R., Graham, M. J., et al. 2019, *PASP*, 131, 018002
- Blagorodnova, N., Neill, J. D., Walters, R., et al. 2018, *PASP*, 130, 035003
- Blondin, S. & Tonry, J. L. 2007, in *American Institute of Physics Conference Series*, Vol. 924, 312–321
- Burrows, D. N., Hill, J. E., Nousek, J. A., et al. 2005, *Space Sci. Rev.*, 120, 165
- Cano, Z. 2013, *MNRAS*, 434, 1098
- Cardelli, J. A., Clayton, G. C., & Mathis, J. S. 1989, *ApJ*, 345, 245
- enko, S. B., Fox, D. B., Moon, D.-S., et al. 2006, *PASP*, 118, 1396
- Chen, T. W., Inserra, C., Fraser, M., et al. 2018, *ApJ*, 867, L31
- Chevalier, R. A. & Fransson, C. 2017, *Thermal and Non-thermal Emission from Circumstellar Interaction*, ed. A. W. Alsabti & P. Murdin, 875
- De, K., Kasliwal, M. M., Ofek, E. O., et al. 2018, *Science*, 362, 201
- Dekany, R., Smith, R. M., Riddle, R., et al. 2020, *PASP*, 132, 038001
- Ergon, M., Jerkstrand, A., Sollerman, J., et al. 2015, *A&A*, 580, A142
- Ergon, M., Sollerman, J., Fraser, M., et al. 2014, *A&A*, 562, A17
- Evans, P. A., Beardmore, A. P., Page, K. L., et al. 2009, *MNRAS*, 397, 1177
- Fransson, C., Chevalier, R. A., Filippenko, A. V., et al. 2002, *ApJ*, 572, 350
- Fransson, C., Ergon, M., Challis, P. J., et al. 2014, *ApJ*, 797, 118
- Fremming, C., Ko, H., Dugas, A., et al. 2019, *ApJ*, 878, L5
- Fremming, C., Sollerman, J., Taddia, F., et al. 2016, *A&A*, 593, A68
- Gal-Yam, A., Arcavi, I., Ofek, E. O., et al. 2014, *Nature*, 509, 471
- Gehrels, N., Chincarini, G., Giommi, P., et al. 2004, *ApJ*, 611, 1005
- Graham, M. J., Kulkarni, S. R., Bellm, E. C., et al. 2019, *arXiv e-prints*
- Groh, J. H., Meynet, G., Georgy, C., & Ekström, S. 2013, *A&A*, 558, A131
- HI4PI Collaboration, Ben Bekhti, N., Flöer, L., et al. 2016, *A&A*, 594, A116
- Hickish, J., Razavi-Ghods, N., Perrott, Y. C., et al. 2018, *MNRAS*, 475, 5677
- Hodgkin, S. T., Breedt, E., Delgado, A., et al. 2019, *Transient Name Server Discovery Report*, 2019-2225, 1
- Houck, J. C. & Fransson, C. 1996, *ApJ*, 456, 811
- Johansson, S. & Jordan, C. 1984, *MNRAS*, 210, 239
- Kuncarayakti, H., Anderson, J. P., Galbany, L., et al. 2018a, *A&A*, 613, A35
- Kuncarayakti, H., Maeda, K., Ashall, C. J., et al. 2018b, *ApJ*, 854, L14
- Lyman, J. D., Bersier, D., James, P. A., et al. 2016, *MNRAS*, 457, 328
- Malesani, D., Fynbo, J. P. U., Hjorth, J., et al. 2009, *ApJ*, 692, L84
- Malesani, D. B., Charalampopoulos, P., Angus, C., Izzo, L., & Yaron, O. 2019, *Transient Name Server Classification Report*, 2019-2284, 1
- Masci, F. J., Laher, R. R., Rusholme, B., et al. 2019, *PASP*, 131, 018003
- Matheson, T., Filippenko, A. V., Ho, L. C., Barth, A. J., & Leonard, D. C. 2000, *AJ*, 120, 1499
- Maund, J. R. & Smartt, S. J. 2009, *Science*, 324, 486
- Mazzali, P. A., Sullivan, M., Pian, E., Greiner, J., & Kann, D. A. 2016, *MNRAS*, 458, 3455
- Milisavljevic, D., Margutti, R., Kamble, A., et al. 2015, *ApJ*, 815, 120
- Nomoto, K., Suzuki, T., Shigeyama, T., et al. 1993, *Nature*, 364, 507
- Oke, J. B., Cohen, J. G., Carr, M., et al. 1994, in *Society of Photo-Optical Instrumentation Engineers (SPIE) Conference Series*, Vol. 2198, *Instrumentation in Astronomy VIII*, ed. D. L. Crawford & E. R. Craine, 178–184
- Perley, D. A. 2019, *PASP*, 131, 084503
- Prentice, S. J., Ashall, C., James, P. A., et al. 2019, *MNRAS*, 485, 1559
- Rigault, M., Neill, J. D., Blagorodnova, N., et al. 2019, *A&A*, 627, A115
- Roming, P. W. A., Kennedy, T. E., Mason, K. O., et al. 2005, *Space Sci. Rev.*, 120, 95
- Schlafly, E. F. & Finkbeiner, D. P. 2011, *ApJ*, 737, 103
- Sigut, T. A. A. & Pradhan, A. K. 1998, *ApJ*, 499, L139
- Sigut, T. A. A. & Pradhan, A. K. 2003, *ApJS*, 145, 15
- Smith, N. 2014, *ARA&A*, 52, 487
- Smith, N., Silverman, J. M., Chornock, R., et al. 2009, *ApJ*, 695, 1334
- Sollerman, J., Taddia, F., Arcavi, I., et al. 2019, *A&A*, 621, A30
- Springob, C. M., Magoulas, C., Colless, M., et al. 2014, *MNRAS*, 445, 2677
- Stritzinger, M., Taddia, F., Fransson, C., et al. 2012, *ApJ*, 756, 173
- Sun, N.-C., Maund, J. R., & Crowther, P. A. 2020, *arXiv e-prints*, [arXiv:2003.09325](https://arxiv.org/abs/2003.09325)
- Taddia, F., Fremming, C., Sollerman, J., et al. 2016, *A&A*, 592, A89
- Taddia, F., Sollerman, J., Leloudas, G., et al. 2015, *A&A*, 574, A60
- Taddia, F., Stritzinger, M. D., Bersten, M., et al. 2018, *A&A*, 609, A136
- Yan, L., Lunnan, R., Perley, D. A., et al. 2017, *ApJ*, 848, 6
- Yaron, O. & Gal-Yam, A. 2012, *PASP*, 124, 668
- Yoon, S.-C. 2015, *PASA*, 32, 15
- Zwart, J. T. L., Barker, R. W., Biddulph, P., et al. 2008, *MNRAS*, 391, 1545

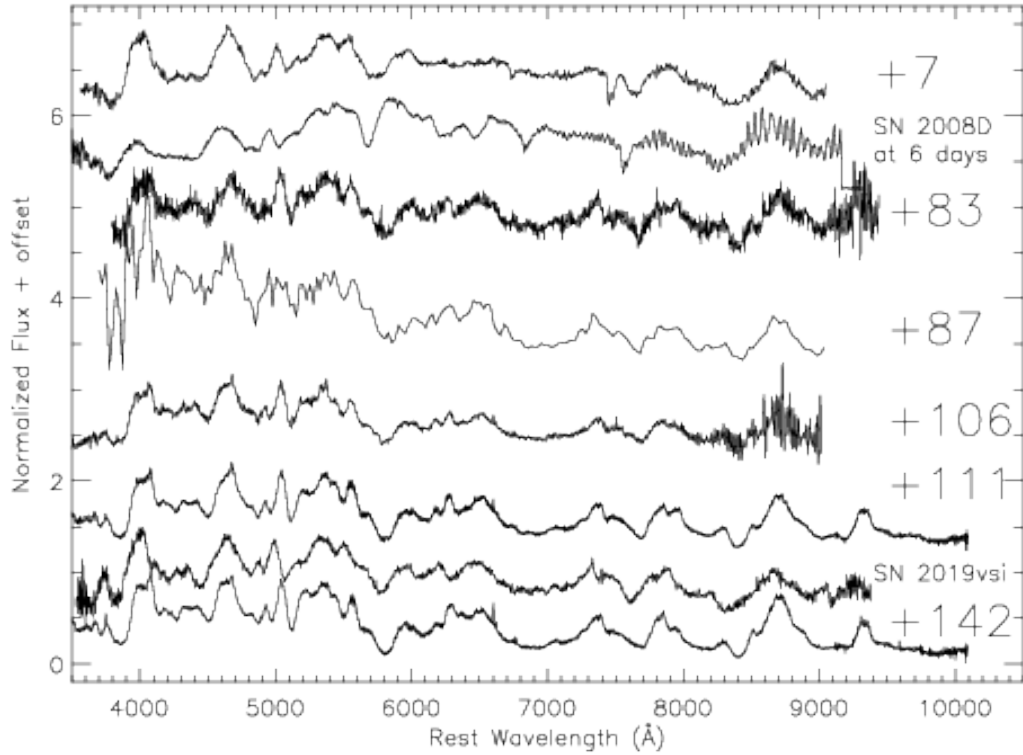


Figure 4: The spectral sequence of SN 2019tsf demonstrates that the spectral evolution is quite slow. We show a selection of the spectra listed in Table 1. Phases given in rest-frame days are provided for each spectrum. The second spectrum from top is of the Type Ib SN 2008D obtained 6 days past maximum light from Malesani et al. (2009). This gives the best match of the classification spectrum using SNID. The spectra obtained at ~ 100 days when the supernova was rebrightening are still quite similar to the typical Type Ib SN spectrum obtained close after discovery. The second to last spectrum is of the Type Ib SN 2019vsi about 80 days past discovery, and shows great similarity with the spectra of SN 2019tsf. No signs of narrow lines or other features signalling CSM interaction can be found, in stark contrast to the case of SN 2019oys. The spectra are normalized and offset for clarity, all data will be made available via WISEREP.

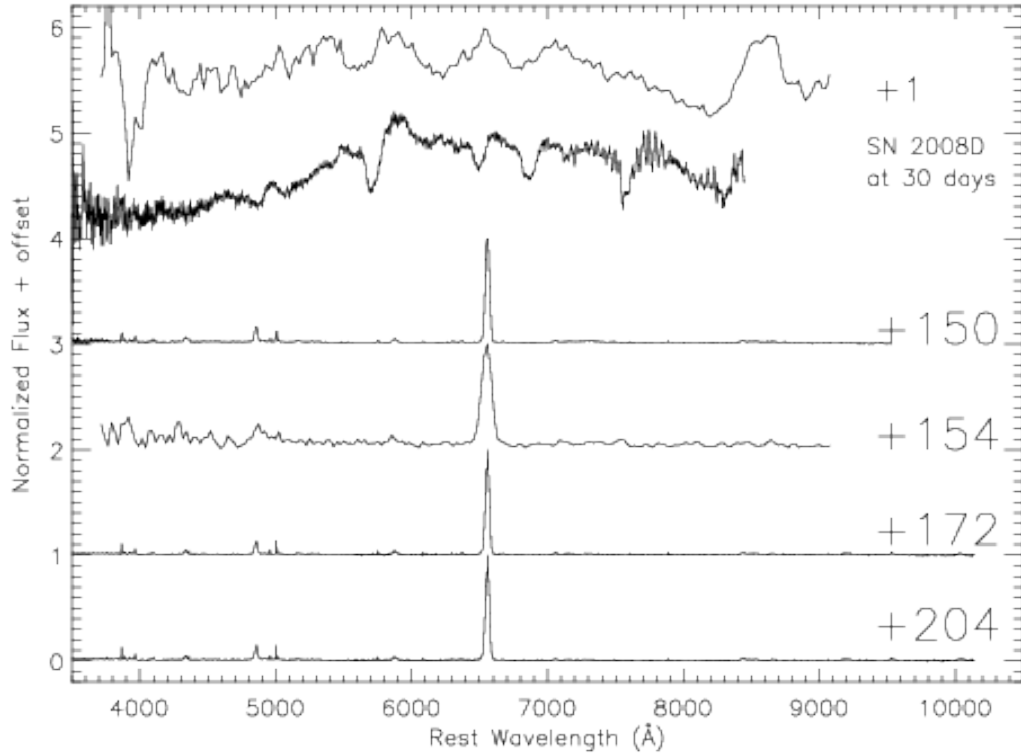


Figure 5: The spectral sequence of SN 2019oys shows an abrupt change from the very first Type Ib spectrum obtained by the P60, to the later spectra acquired once the light curve started to brighten. These latter spectra show clear evidence for CSM interaction as evidenced by the dominance of the narrow emission lines. We show a selection of the spectra listed in Table 1 for this supernova. Phases in rest-frame days are provided for each spectrum. The second spectrum from the top is of the Type Ib SN 2008D, which gives the best match of the classification spectrum using SNID at 30 days past maximum light. This spectrum is from Malesani et al. (2009). The spectra obtained at $\gtrsim 150$ days when the supernova was re-brightening are quite similar to the spectra of the Type IIn SN 2015ip and this is highlighted in Fig. 6. The spectra are normalized and offset for clarity, all data will be made available via WISEREP.

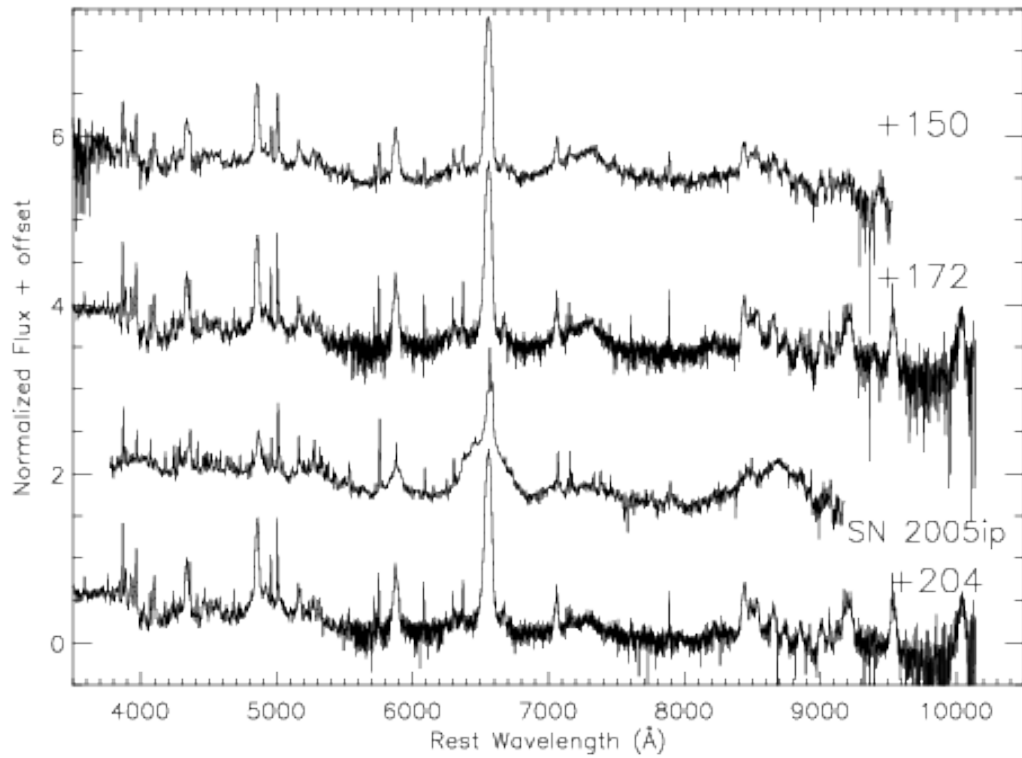


Figure 6: Spectral sequence of SN 2019oys during rebrightening. A handful of the spectra listed in Table 1 are shown, and this time in logarithmic scale to highlight the bright narrow emission lines. Phases in rest-frame days are provided for each spectrum. A spectrum of the Type II_n SN 2015ip is shown for comparison. This spectrum is from [Stritzinger et al. \(2012\)](#) taken at 138 days past discovery. Basically all high excitation coronal lines seen in SN 2005ip are also detected in SN 2019oys, a main difference being that our SN do not display the broad H α line from hydrogen-rich ejecta. The spectra are normalized and offset for clarity.

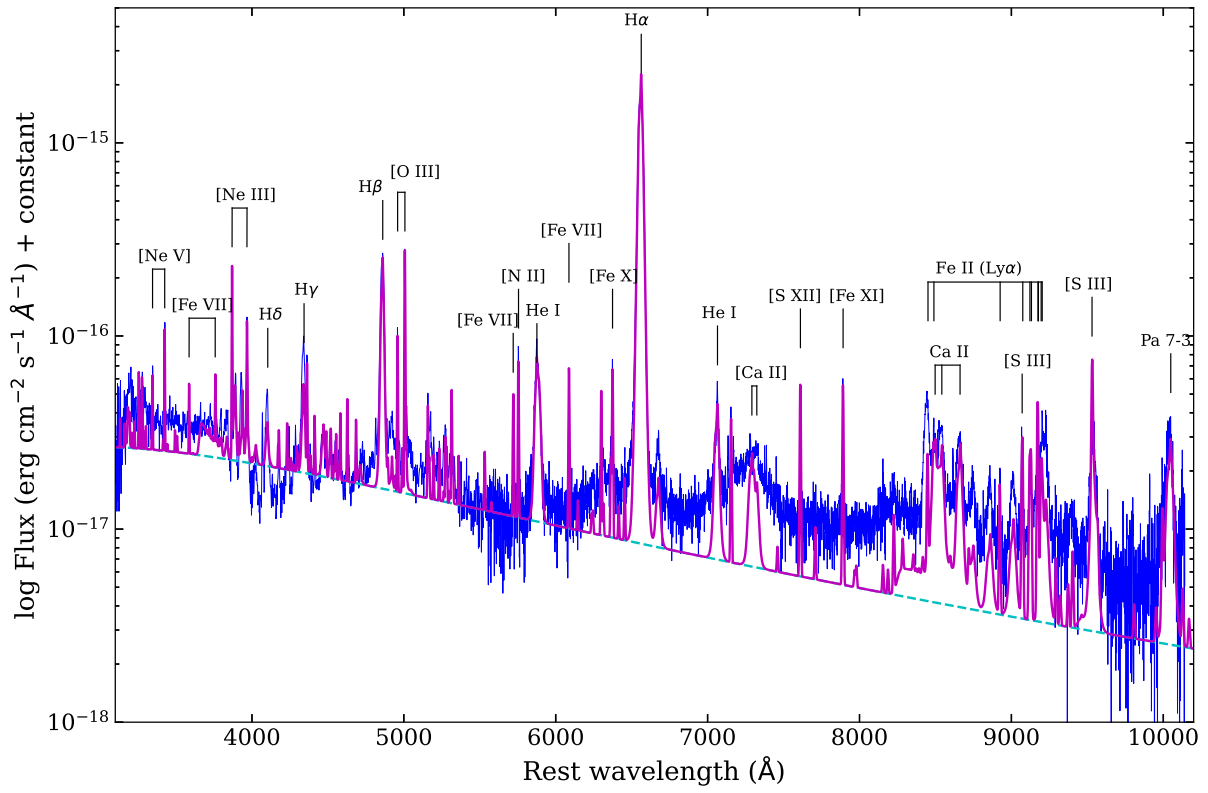


Figure 8: Synthetic spectrum (magenta) together with the reddening corrected spectrum of SN 2019oys from day 172 (blue) with line identifications. The assumed blackbody continuum is shown as the dashed cyan line.

Table 1. Summary of Spectroscopic Observations

Object	Observation Date (YYYY MM DD)	Phase (Rest-frame days)	Telescope+Instrument
SN 2019tsf	2019 Nov 05	6.71	NTT+EFOSC2 ^a
SN 2019tsf	2020 Jan 21	82.9	NOT+ALFOSC
SN 2019tsf	2020 Jan 26	87.0	P60+SEDM
SN 2019tsf	2020 Feb 02	93.8	P60+SEDM
SN 2019tsf	2020 Feb 07	98.7	P60+SEDM
SN 2019tsf	2020 Feb 15	106.4	TNG+DOLORES
SN 2019tsf	2020 Feb 19	110.6	Keck1+LRIS
SN 2019tsf	2020 Mar 22	141.9	Keck1+LRIS
SN 2019tsf	2020 Apr 28	178.7	NOT+ALFOSC
SN 2019oys	2019 Aug 29	0.96	P60+SEDM
SN 2019oys	2020 Jan 27	150.0	NOT+ALFOSC
SN 2019oys	2020 Feb 01	154.1	P60+SEDM
SN 2019oys	2020 Feb 09	162.2	P60+SEDM
SN 2019oys	2020 Feb 15	166.6	NOT+ALFOSC
SN 2019oys	2020 Feb 19	172.0	Keck1+LRIS
SN 2019oys	2020 Feb 24	176.8	P60+SEDM
SN 2019oys	2020 Mar 22	203.5	Keck+LRIS
SN 2019oys	2020 Apr 15	227.0	P60+SEDM
SN 2019oys	2020 May 01	243.3	NOT+ALFOSC

^aThis spectrum is from TNS provided by Malesani et al. (2019).

Table 2: SN 2019oys - radio observations

Δt [Days]	Frequency [GHz]	F_ν [mJy/beam]	Image RMS [mJy]	Telescope
21.9	15.5	0.35 ± 0.05	0.04	AMI-LA
25.7	15.5	0.37 ± 0.05	0.04	AMI-LA
191	15.5	9.08 ± 0.5	0.06	AMI-LA
198	15.5	10.0 ± 0.5	0.06	AMI-LA
201	23.5	21.5 ± 1.0	0.05	VLA
204	15.5	10.3 ± 0.5	0.05	AMI-LA

Table 3. Fluxes of Selected Narrow/Coronal Lines in SN 2019oys

Line ID	Intrinsic λ (Å)	Measured λ (Å)	Flux (10^{-16} erg s $^{-1}$ cm $^{-2}$)	FWHM (Å)	
[Ne v]	3346	3345.9	2.6	6.9	blended with [Ne III] 3342 ?
[Ne v]	3426	3426.5	4.7(0.5)	5.0	
[Fe VII]	3586	3586.9	1.3(0.2)	4.5	
[O II]	3727	3725.8	0.46	4.4	very weak
[Fe VII]	3759	3759.4	1.9	6.4	
[Ne III]	3869	3868.9	11.4	4.99	strong and narrow
[He I]	3889	3889.6	8.4	18	Two broader lines between the Ne III line
[Ca II]		3932.0	10.9	22	? Broad Potentially Ca 3933 if 3968 blended
[Ne III]	3968	3967.5	9.1	9.4	Likely somewhat contaminated by He I
[Fe V]	4072	4069.3	2.1	7.4	Not in Claes Figure
H δ	4103	4100	9.5	22	Broad
[Ni XII]	4232	...			There is a blend there, likely also something
H γ	4340	4338.1	15.1	21	Broad with structure
[O III]	4363	4362.72	4.0(0.7)	4.8	Narrow
[Ar XIV]	4412	4415.4	1.4	7.1	
[He II]	4686	4685.9	1.8	7.8	as strong as previous line, not in Smith Table
() H β	4861	4858.6	69.0	26	
[Fe IV]	4906	4905.3	0.36	4.1	Not strong = Hardly detected
He I	4922				Blended and weak if present
[O III]	4959	4958.9	5.1	5.1	
[O III]	5007	5006.82	15.6	5.2	
[Fe VII]	5158	5159.0	1.5	5.4	
[Fe VI]	5176	5174.7	2.6	13	Weak and blended, but present
[Fe VII]	5276	5274.9	1.4	10.5	
[Fe XIV],[Ca V]	5303,09				Not strong
[Fe II]	5328				Not Strong
[Ar X]	5536				Not Strong (but clear in Claes figure)
[Fe VII]	5720	5720.8	1.57	5.3	
[N II]	5755	5754.3	4.43	5.1	
He I	5876	5878.1	25.1	35	Triangular, strong 6678 is there but 4471 is not
[Fe VII]	6086	6086.25	2.30	5.1	
[O I]	6300	6299.8	1.62	5.1	
[S III]	6312				Present but weak
[O I]	6364	6364.1	1.1	7.9	Somewhat blended
[Fe X]	6375	6373.6	3.41	5.5	
H α	6563	6560.0	714	34.6	Not in Smiths Table for some reason, could be
He I	6680	6675.0	3.94	25.3	Broad, no narrow component
[S II]	6717				Not there!
[S II]	6731				Not there!
He I (Nar.)	7065	7064.0	4.9	9.0	Narrow peak of line
He I (Tot.)	7065	7062.6	11.1	34.2	Total
[Ar III]	7136	7135.2	1.55	10.2	
[Fe II]	7155	7154.4	1.81	6.4	Narrow
X X XX	7171.8	0.77	8.9		Not strong, but perhaps something
He I	7281	7281.48	0.68	9.4	Not significantly detected
[O II]	7325				Not detected
[S XII]	7611	7608.5	1.56	6.7	
[Fe IV]?	7704				no
[Fe XI]	7891	7890.8	2.30	4.44	
He I	8232	8227.4	0.36	6.3	Hardly significant
He I	8295				No
O I	8446	8443.4	14.1	35.5	Strong Broad
Ca II	8498,8542,8662 ??	8443.4,8534.52,8658.99		42	Strong Broad features, Not in SN 2005ip
[Fe VII]	8729				No
[S III]	9069	9069.55	2.11	10.4	
[Fe II]	XX	8489.5, 8616.3, 8892.0, 8925.8 9175.9,			Narrow lines not in Smith et al. Are these
[S III]	9531	9530.5	2.79	5.3	Narrow and Strong, not in Smith et al.
Pashen8	9546	9535.8	12.0	35	Broad + Narrow
Pashen7	10036.7	20.9	74		Broad at end of sensitivity

Note. — Fluxes are given in units of 10^{-16} erg s $^{-1}$ cm $^{-2}$. These are NOT YET corrected for extinction and reddening of $E(B - V) = 0.0XX$ mag in the Milky Way, but not for extinction local limit is in parentheses when no measurement is given. Listed uncertainties are 1σ based on the adjacent continuum noise, although the true uncertainties may be higher for blended lines. *These are on this and will re-measure all lines. Also need to synch with the Line IDs of Claes and that discussion.*